Proceedings of HT2005
2005 ASME Summer Heat Transfer Conference
July 17-22, 2005, San Francisco, California, USA

HT2005-72377

MONTE CARLO SIMULATION OF THERMAL CONDUCTIVITIES OF SILICON NANOWIRES

Yunfei Chen
Department of Mechanical Engineering and China Education Council Key Laboratory of MEMS, Southeast University, Nanjing, 210096, P. R. of China

Deyu Li
Department of Mechanical Engineering, Vanderbilt University, Nashville TN, 37235-1592

Jennifer R. Lukes
Department of Mechanical Engineering and Applied Mechanics, University of Pennsylvania, Philadelphia PA 19104-6315

Zhonghua Ni
Department of Mechanical Engineering and China Education Council Key Laboratory of MEMS, Southeast University, Nanjing, 210096, P. R. of China

ABSTRACT

One-dimensional (1D) materials such as various kinds of nanowires and nanotubes have attracted considerable attention due to their potential applications in electronic and energy conversion devices. The thermal transport phenomena in these nanowires and nanotubes could be significantly different from that in bulk material due to boundary scattering, phonon dispersion relation change, and quantum confinement. It is very important to understand the thermal transport phenomena in these materials so that we can apply them in the thermal design of microelectronic, photonic, and energy conversion devices. While intensive experimental efforts are being carried out to investigate the thermal transport in nanowires and nanotube, an accurate numerical prediction can help the understanding of phonon scattering mechanisms, which is of fundamental theoretical significance. A Monte Carlo simulation was developed and applied to investigate phonon transport in single crystalline Si nanowires. The Phonon-phonon Normal (N) and Umklapp (U) scattering processes were modeled with a genetic algorithm to satisfy both the energy and the momentum conservation. The scattering rates of N and U scattering processes were given from the first perturbation theory. Ballistic phonon transport was modeled with the code and the numerical results fit the theoretical prediction very well. The thermal conductivity of bulk Si was then simulated and good agreement was achieved with the experimental data. Si nanowire thermal conductivity was then studied and compared with some recent experimental results. In order to study the confinement effects on phonon transport in nanowires, two different phonon dispersions, one based on bulk Si and the other solved from the elastic wave theory for nanowires, were adopted in the simulation. The discrepancy from the simulations based on different phonon dispersions increases as the nanowire diameter decreases, which suggests that the confinement effect is significant when the nanowire diameter goes down to tens nanometer range. It was found that the U scattering probability engaged in Si nanowires was increased from that in bulk Si due to the decrease of the frequency gap between different modes and the reduced phonon group velocity. Simulation results suggest that the dispersion relation for nanowire solved from the elasticity theory should be used to evaluate nanowire thermal conductivity as the nanowire diameter reduced to tens nanometer

INTRODUCTION

In recent years, low-dimensional structures have attracted much attention for their potential application in thermoelectric devices. The performance of thermoelectric devices depends on the figure of merit ZT, given by

$$ZT = (\alpha^2 T / \rho K_T) \qquad (1)$$

where α, T, ρ, K_T are the Seebeck coefficient, absolute temperature, electrical resistivity and total thermal conductivity, respectively. For a material to have a high ZT, one requires a high thermoelectric power α (Seebeck coefficient), a low electrical resistvity and a low thermal conductivity. A material with a figure of merit of around 1.0 was first reported over four decades ago, but since then, little progress has been made in finding new materials with enhanced

ZT values at room temperature [1]. A big challenge to enhance the ZT value is to decrease the thermal conductivity and at the same time not to produce a deterioration of electronic transport. Nanostructures such as nanowires and quantum wells provide a promising method for the enhancement of ZT through controlling the phonon and electron transport [2].

Phonon transport at the nanoscale differs from that at the macro- and microscale for several fundamental reasons. One is that size confinement changes the phonon dispersion relation. This change causes the phonon group velocity to differ from that in bulk material. A more complicated problem is that the phonon scattering rate also differs from that in bulk material [3]. This affects the phonon mean free path, which in turn changes the lattice thermal conductivity of the nanostructure. In addition, as the size of the nanostructure decreases below the phonon mean free path and starts to approach the wavelength of the dominant phonon, λ, the validity of phonon particle transport theory becomes questionable and wave theory should be applied to interpret heat transport in nanostructures. So far there are two distinct methods for the analysis of heat conduction in nanowires. Those include the solution of the Boltzmann transport equation (BTE) and the molecular dynamics simulation method. Based on the lifetime assumption and accounting for the modified nanowire acoustic phonon dispersion relation, it is possible to predict nanowire thermal conductivity [4-8] from the solution of the BTE. Because great simplifications must be introduced to produce a closed form solution, the results usually deviate greatly from experimental findings. Certain assumptions lead to erroneous explanations of particular phenomena [9]. The molecular dynamics simulation method uses Newton's second law to describe the movement of a large number of atoms in the nanowire. Thermal conductivity can be extracted from averaging the positions and velocities of the atoms [10]. However, this method is limited by the knowledge of interatomic potential and computation ability.

In this paper, the Monte Carlo simulation method is used to trace the phonon movement in a Si nanowire. Three phonon scattering, boundary scattering and impurity scattering processes are considered. A genetic algorithm is used to guarantee energy and wave-vector conservation conditions for N and U scattering. Bulk silicon and silicon nanowire thermal conductivities are calculated. Simulation results agree well with that from previous investigations and experimental results.

II. OVERVIEW OF MONTE CARLO METHOD

The Boltzmann equation for phonon transport in the presence of a temperature gradient is written as

$$\vec{V}_g \bullet \nabla T \frac{dN}{dT} = (\frac{\partial N}{\partial t})_c \qquad (2)$$

where $\vec{V}_g$ is the group velocity, $\vec{V}_g = \nabla_{\vec{K}} \omega$, (3)

N is the distribution function, $\vec{K}$ is the phonon wavevector, T is local temperature, ω is the phonon frequency, and $(\frac{\partial N}{\partial t})_c$ is the rate of change of N due to collision. On the left side of equation (2) N can be replaced by N_0, the equilibrium Planck distribution. Consequently equation (3) can be read as

$$\vec{V}_g \bullet \nabla T \frac{dN_0}{dT} = \sum_{K'} [\Phi(K, K')N(K') - \Phi(K', K)N(K)] \qquad (4)$$

where $N_0 = \dfrac{1}{\exp(\hbar\omega / k_B T) - 1}$ (5)

$\hbar$ is the Planck constant divided by 2π, k_B is the Boltzmann constant, and $\Phi(K, K')$ is the function describing the scattering rate from state K' to state K, which depends on the phonon frequency and polarization.

Equation (4) is a nonlinear integro-differential equation. Without simplification the formulation is difficult to solve. This difficulty can be avoided by using the Monte Carlo method. This method does not consider equation (4) directly but instead follows a large number of phonons in a three-dimensional space subjected to a temperature gradient to simulate thermal properties. The simulation starts with all of the phonons in given initial conditions with the appropriate sampled frequency, group velocity, wavevector and polarization, after which the duration of the free flight is set and all of the phonons move linearly from the initial to new positions such that

$$\vec{r}_i = \vec{r}_{0,i} + \vec{V}_{g,i} \Delta t \qquad (6)$$

where $\vec{r}_i, \vec{r}_{0,i}$ are the phonon's new and initial position respectively, and Δt is the free flight time. The free flight time is kept constant during the simulation. If the phonon encounters a boundary during free flight, it is reflected as described in the next section. Following the free flight, scattering mechanisms are imposed. Each phonon has its own unique lifetime τ_T based on its frequency, polarization, impurity scattering time scale and local temperature [6]. $P(t)$, the probability that a phonon has already lived for the free flight time Δt without being scattered, decreases in time such that

$$\frac{\partial P}{\partial t} = -\frac{P}{\tau_T} \qquad (7)$$

and after the free flight time, the probability of scattering is

$$\overline{P} = 1 - \exp(-\Delta t / \tau_T). \qquad (8)$$

To impose a statistical scattering mechanism on the phonons, a random number R is generated. If $R < \overline{P}$, the phonon will be scattered and replaced by a new phonon of a different state. This new state is determined using the genetic algorithm described below. Then the new phonon begins its new free flight. If $R > \overline{P}$, the phonon will continue its free flight with its state unchanged. For long enough simulation times, the system equilibrates and the final results can be extracted through averaging over a fixed time step.

III. Scattering mechanisms

During phonon transport, phonon scattering usually involves either boundary collisions, impurity scattering, or three phonon inelastic interactions. Boundary collisions play an important role in thermal resistance as the structure size decreases to the nanoscale. When a phonon strikes the structure wall, a random number is first drawn. If this random number is

less than a prescribed specular parameter d, the phonon is specularly reflected using the relation [12]

$$\vec{s}_r = \vec{s}_i + 2|\vec{s}_i \bullet \vec{n}|\vec{n} \tag{9}$$

where $\vec{s}_i, \vec{s}_r$ are the direction vectors of the incident and reflected phonon. If the random number is larger than d, the phonon is reflected diffusely at the surface. Its direction is selected according to the following relation

$$\vec{s}_r = \sin\theta\cos\varphi\vec{t}_1 + \sin\theta\sin\varphi\vec{t}_2 + \cos\theta\vec{n} \tag{10}$$

where $\varphi = 2\pi R_2, \cos\theta = 2R_1 - 1$, R_1, R_2 are random numbers, $\vec{n}$ is the unit surface normal, and $\vec{t}_1, \vec{t}_2$ are unit surface tangents which must be perpendicular to each other such that

$$\vec{t}_1 \times \vec{t}_2 = \vec{n} \tag{11}$$

Impurity scattering contributes greatly to thermal resistance at low temperatures. The time scale for scattering by impurities is expressed using a simple model by Vincenti and Kruger [11]

$$\tau_i^{-1} = B_i\omega^4 \tag{12}$$

where B_i is a constant. Three phonon interactions include both normal (N) and Umklapp scattering processes. For silicon, the inverse lifetimes are as follows [6]

$$\tau_{LNU}^{-1} = B_L\omega^2T^3 \tag{13}$$

$$\tau_{TN}^{-1} = B_{TN}\omega^4 \qquad (TA, Normal)$$

$$\tau_{TU}^{-1} = \begin{cases} 0 & (\omega < \omega_{12}) \\ B_{TU}\omega^2/\sinh(\dfrac{\hbar\omega}{k_BT}) & (\omega \geq \omega_{12}) \end{cases} \tag{14}$$

Equation (13) is the inverse lifetime for the longitudinal phonons to engage in the N and U scattering processes. For the transverse phonons Eq. (14) shows that the U scattering processes would not begin until $\omega \geq \omega_{12}$, where ω_{12} is the transverse branch frequency corresponding to $K/K_{\max} = 0.5$. Peierls[13] showed that N processes contribute to thermal resistance by transferring momentum from one group of modes, where resistance (R) processes (Umklapp or impurity processes) are weak, to other modes where R processes are strong. This effect is particularly important for point defect scattering, since the scattering probability is strongly frequency dependent. The total phonon lifetime in Eqs. (12-14) can thus be constructed using the Matthiesen rule:

$$\frac{1}{\tau_T} = \frac{1}{\tau_R} + \frac{1}{\tau_N} \tag{15}$$

where

$$\frac{1}{\tau_R} = \frac{1}{\tau_i} + \frac{1}{\tau_U} \tag{16}$$

Callaway [5] assumed that N processes relax towards a quasiequilibrium distribution, i.e., one shifted in momentum space, while R processes tend to restore true equilibrium. The shift of the quasiequilibrium distribution is chosen so that N processes conserve momentum in the aggregate. The displaced Planck distribution can be written as [5]

$$N(\vec{\lambda}) = [\exp(\frac{\hbar\omega - \vec{\lambda}\bullet\vec{K}}{k_BT})]^{-1} = N_0 + \frac{\vec{\lambda}\bullet\vec{K}}{k_BT}\frac{e^{\hbar\omega/k_BT}}{(e^{\hbar\omega/k_BT}-1)^2} \tag{17}$$

where $\vec{\lambda}$ is a constant vector in the direction of the temperature gradient. Based on the Callaway model, Armstrong proposed a two fluid model to make additional corrections [14] but equation (17) is appropriate for the Monte Carlo simulation. Using formula (17), the departure of the phonon occupation number from thermal equilibrium at small vector interval can be written as

$$\Delta N = \iiint_{\Delta K}(N(\vec{\lambda}) - N)d^3K = \sum_{K_X}^{K_x+\Delta K_x}\sum_{K_y}^{K_y+\Delta K_y}\sum_{K_z}^{K_z+\Delta K_z}(N(\vec{\lambda}) - N)\Delta K_x\Delta K_y\Delta K_z \tag{18}$$

The three phonon interactions obey the energy conservation and momentum conservation laws:

$$K_1 + K_2 \leftrightarrow K_3 \tag{19}$$

$$K_1 + K_2 \leftrightarrow K_3 + G \tag{20}$$

$$\omega_1 + \omega_2 = \omega_3 \tag{21}$$

where G is the reciprocal lattice vector. Eq. (19) represents momentum conservation for normal processes while Eq. (20) represents momentum conservation for Umklapp processes. In order to satisfy equations (18-21) simultaneously, a genetic algorithm is introduced to conserve momentum and energy:

$$Min: r_1 = \sum_{i=1}^{N_c}(\frac{K_{x,i}^{'} - K_{x,i}}{K_{x,i}})^2 + (\frac{K_{y,i}^{'} - K_{y,i}}{K_{y,i}})^2 + (\frac{K_{Z,i}^{'} - K_{Z,i}}{K_{Z,i}})^2 \tag{22}$$

$$Min: r_2 = (\sum_{i=1}^{N_c}\omega_i^{'} - \sum_{i=1}^{N_c}\omega_i)^2/(\sum_{i=1}^{N_c}\omega_i)^2 \ . \tag{23}$$

Here N_c is the number of phonons to be scattered, $K_{x,i}^{'}, K_{y,i}^{'}, K_{z,i}^{'}, \omega_i^{'}$ are the new phonon's *x*, *y* and *z* direction wave vectors and frequency, and $K_{x,i}, K_{y,i}, K_{z,i}, \omega_i$ are the corresponding phonon state quantities before scattering. r_1 and r_2 are residuals of the wave vector and frequency, and in our algorithm they are set as 0.001. In the optimization process, the new quantities can be set to zero to represent a phonon deleted from the simulation domain. An N-type scattering process should satisfy conditions (22) and (23), while an R process should satisfy conditions (23) only. The genetic algorithm is operated as follows:

1. Scattered phonons: Put all of the scattered phonons in a group, $S = \{s_i | i = 1,..., N_c\}$, where N_c is the number

of the phonons to be scattered in a time step. s_i represents the phonon to be scattered.

2. Initialization: Generate an initial set $F = \{f_1, f_2, ..., f_n\}$ of individuals according to local temperature and equation (17), where in every individual there are N_c phonons produced. Set the initial set as father generation.
3. Reproduction: Based on the father generation, reproduce the offspring generation $S = \{s_1, s_2, ..., s_n\}$. In this step a crossover operation is used to produce the offspring generation. The crossover operation produces the offspring by randomly exchanging individuals between the father generation. For example, we can use f_1, f_2 to represent a father generation, and 0,1 to represent the individual phonons such that $\begin{cases} f_1 = [0,0,1,0,...,1,\underline{1},\underline{0},\underline{1}] \\ f_2 = [1,0,1,0,...,0,\underline{0},\underline{0},\underline{1}] \end{cases}$. From the father generation, an offspring s_i can be produced by exchanging the underlined phonons and retaining the others so that $s_i = [0,0,1,0,...,1,0,0,1]$ is produced.
4. Initial evaluation: Evaluate all individuals and calculate their fitness according to equations (17), (18), (22) and (23).
5. Selection: Choose the best individual $f_{best} \in F \cup S$.
6. Mutation: From the best individual generate a set of n/2 mutants: $M = \{s_i' := mut(s_{best}) \mid i = 1,2,...,n/2\}$. In this operation, n/2 phonons will be selected randomly according to the equilibrium distribution. For example, if $s_i = [0,0,1,0,...,\underline{1},\underline{1},\underline{0},0]$, after the mutation operation $s_i' = [0,0,1,0,...,0,0,1,0]$ will be produced.
7. Generate new generation: Evaluate the fitness of the individuals in M and select n individuals from M, S, F according to their fitness to generate a new generation F, i.e. $F \subset (M \cup S \cup F)$.
8. Evaluation: Evaluate all individuals in F and calculate their fitness.
9. Terminate check: If at least one of the individuals has achieved the predefined fitness, stop and return the best individual. Otherwise, continue with step 3.

In this algorithm the optimization object is to satisfy $r_1 < 0.001$ for U scattering processes or $r_1 + r_2 < 0.001$ for N scattering processes. Impurity scattering processes are disposed in the same way as the U scattering process. The N and U scattering processes are treated in different steps, but all of the phonons engaged in the same scattering processes are considered together to satisfy the energy conservation and momentum conservation law. Although this is an approximate method to handle the three-phonon interactions, it is still a time consuming algorithm.

V. Numerical results

A silicon nanowire is simulated by the Monte Carlo method using the algorithm described above. The structure of the silicon nanowire is shown in Fig.1. The cross section of the nanowire is a square of dimension *a*. The bulk dispersion relation for silicon shown in Fig. 2 is adopted for this model.

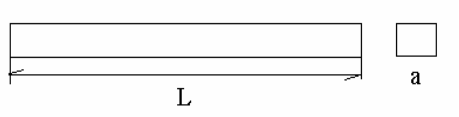

Figure 1. Structure of Si nanowire

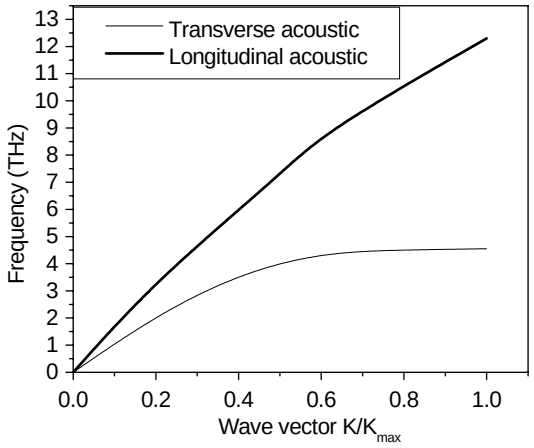

Figure.2 Dispersion relation for Si

Figure 3 gives the temperature profile for the case of ballistic transport. At low temperature if the impurity and boundary scattering processes are not taken into account the phonons will transport without engaging in any scattering processes and their mean free path will be infinite. In this case there is no thermal resistance and the temperature remains constant according to the following formula

$$T^4 = (T_L^4 + T_R^4)/2 \qquad (24)$$

Where T_L, T_R stand for the temperature at the two ends. From Fig. 3 it can be found that the numerical results agree well with the above formula.

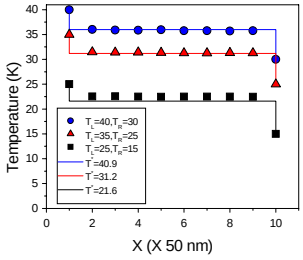

Figure 3 Temperature distribution under ballistic condition in a Si nanowire, T_L, T_R correspond to the temperature on the left and right ends, and T^* is given by equation (24)

If the prescribed value d is set as 1.0, the boundary surfaces are perfectly smooth and diffuse scattering off boundaries does not arise. All of the phonons are specularly

reflected when they hit the walls. In this case the thermal conductivity of the nanowire is equal to the bulk thermal conductivity. Figure 4 illustrates the thermal conductivity of bulk Si as a function of temperature. The numerical results for a nanowire with $d = 1$ agree well with previous experimental results[6] for temperatures greater than 150 K, demonstrating that the Monte Carlo simulation method works well at those temperatures. For $T < 25K$, the Monte Carlo results deviate from the experimental data. Experimental conductivities are limited by grain size in the sample. The polycrystallinity of the bulk sample is why thermal conductivity goes down at low temperatures even though the sample is supposed to be 'infinite'. The MC calculation neglects the boundary scattering process, which is dominant below 25K. This explains the increase of simulated thermal conductivity toward infinity shown in Figure 4. In order to match experimental results for Si nanowires, the parameter *d*, which describes the boundary scattering process probability, is calibrated.

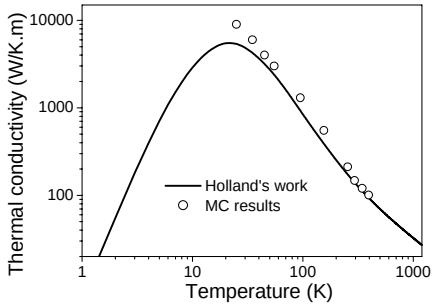

Figure 4. Thermal conductivity of bulk Si at different temperatures (the word Experiment is misspelled in Fig 4)

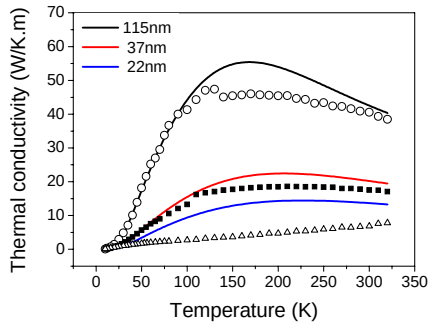

Figure 5. Thermal conductivity of Si nanowires with different diameters

Figure 5 illustrates the thermal conductivity temperature dependence of Si nanowires with different diameters. The three solid lines stand for MC simulation results for thermal conductivity of nanowires with diameter 115 nm, 37 nm and 22 nm respectively. The dots represent experimental results. The experimental setup was described in another paper[16]. The MC simulation results agree well at low temperature with the experimental results for nanowire with diameter 37nm and 115 nm. The position of the peak thermal conductivity for the nanowires is displaced to higher temperatures as compared with bulk material at 25K, and it decreases with nanowire dimension. This is attributed to the boundary scattering process. An interesting phenomenon is that with decreasing nanowire diameter, the deviation point between the MC simulation and the experimental results appears earlier on the temperature axis. The deviation begins at T=130K, 100K and 40 K for nanowire diameters 115nm, 37nm and 22nm, respectively. This deviation is not likely caused by the handling of boundary scattering in the MC simulation; as discussed earlier, MC simulations show good agreement with experiment at low temperatures where boundary scattering dominates. When the temperature is over 40K, the N and U scattering processes appear. It is postulated here that N and U scattering processes in the nanowire differ from those in bulk material. In order to verify this idea, closed form solutions for nanowire are used to calculate the thermal conductivity. The calculation procedure is similar to that introduced in reference [17].

$$k^{nanowire} = (\frac{k_B}{\hbar})^3 \frac{k_B}{2\pi^2 V} T^3 \int_0^{\theta_D/T} \frac{\tau_C x^4 e^x}{(e^x - 1)^2} dx \quad (25)$$

where V is the phonon equivalent group velocity, $\tau_C^{-1} = \tau_U^{-1} + \tau_B^{-1} + \tau_I^{-1}$ is the resistive scattering rate, and *T* is the temperature. In formula (25), two types of parameters are used to calculate nanowire thermal conductivity. One set is from bulk Si and the other set is obtained according to the phonon dispersion relation of nanowire.

The Umklapp scattering rate for a nanowire [18] is read as

$$\tau_U^{-1} = \frac{2\gamma^2 \hbar}{3\pi^2 \rho v^2 v_g} \omega_i \omega_j (\omega_i + \omega_j) * [N(\omega_i) - N(\omega_i + \omega_j)] * \int_{q_j} dS' \quad (26)$$

where γ is the Grüneisen parameter, v is the sound velocity, and $N(\omega_i), N(\omega_i + \omega_j)$ are the equilibrium occupations of mode K_i, K_j. Formula (26) describes the relaxation rate of a combining U process as described in equation (20). $v_g = \left\| \partial\omega(q'') / \partial q'' \right\|$ is the group velocity at $\omega'' = \omega_i + \omega_j$ in the longitudinal mode in the principal directionand. The factor $\int_{q_j} dS'$ is the area of the momentum space of the interacting mode K_j with the reference mode K_i. In order to obtain the scattering rate for the U process at mode of K_i, all of the possible interacting channels must be taken into account, then those scattering rates should be summed together.

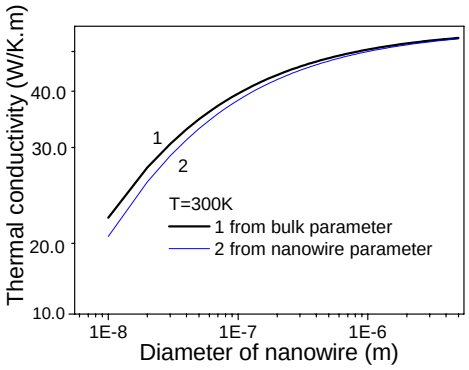

Figure 6 Thermal conductivity of nanowire obtained from different parameters

Figure 6 gives the thermal conductivity for different diameter nanowire by the closed form solutions under different parameter. With increasing of nanowire diameter, the two curves run together. When the diameter is below 100nm, a clear difference can be observed. This can be explained according to formula (25). The thermal conductivity is proportional to the lifetime and is inversely proportional to the phonon group velocity. The equivalent phonon group velocity for nanowire is smaller than that for bulk material and the phonon lifetime evaluated from (26) is also smaller than that obtained by the formula for bulk material. The latter effect is stronger, however, so the net result is that nanowire thermal conductivity is reduced relative to that calculated from the formula for bulk material thermal conductivity.

In conclusion, the Monte Carlo simulation method is used in conjunction with a genetic algorithm to simulate phonon transport in a nanowire. The investigation shows that MC results for nanowires with diameter 37 nm or above agree well at low temperature with the experimental results. For nanowire diameters below 37nm, the nanowire phonon dispersion relation should be used to predict lattice thermal conductivity. An interesting point is that the MC method accounts for acoustic phonon dispersion in each phonon movement. With the phonon scattering rate known, the thermal conductivity of a nanowire can be calculated precisely from its phonon dispersion relation.Put nomenclature here.

ACKNOWLEDGMENTS

This work was supported by NSF. Y.C. also acknowledges the financial support of the Chinese Natural Science Foundation (50276011) and the Hwaying Education Foundation. References

REFERENCES

1. D.A. Wright, Nature 181,834(1958).
2. L.D.Hicks, T.C. Harman, and M.S.Dresselhaus, Appl. Phys. Lett., 63(23), 3230, 1993.
3. A.Khitun and K.L.Wang, Appl. Phys. Lett. 79(6), 851, 2001.
4. P.G. Klemens, Solid state physics, Vol.7, 1958, Academic Press, NY.
5. J. Callaway, Phys. Rev. 113,1046 (1959).
6. M.G. Holland, Phys. Rev. 132,246(1963).
7. B.H. Armstrong, Phys. Rev. B., 32,3381(1985).
8. G. Chen, Phys. Rev. Letters,86,2297 (2001)
9. Y.S. Ju, K.E. Goodson, Applied Physics Letters, 14,3005 (1999).
10. S.G. Volz and G. Chen, Appl. Phys. Lett., 75, 2056, 1999.
11. W.G. Vincenti and C. H. Kruger, Introduction to Physical Gas Dynamics, Robert Krieger Publication, New York, 1977.
12. Sandip Mazudar, Arun Majumdar, Journal of Heat Transfer, 123, 749, 2001.
13. R.E. Peierls, Quantum theory of solids, Oxford University Press, Oxford, 1955.
14. B.H. Armstrong, Phys. Rev. B., 32,3381(1985).
15. M. Asen-Palmer, K. Bartkowski, E. Gmelin, etc, Phys. Rev. B., 56, 9431 (1997).
16. DeYu Li, A.Majumdar, etc, submitted to Phys. Rev. Lett., 2002.
17. Z Jie, A. Bakandin, Journal of Applied Physics, 89(5),2932,2001
18. Y.-J. Han and P.G. Klemens, Phys. Rev. B 48, 6033, 1993.